

Magnetic recoverable $\text{Ag}_3\text{PO}_4/\text{Fe}_3\text{O}_4/\gamma\text{-Fe}_2\text{O}_3$ nanocomposite

Jenifer Vaswani Reboso^{1,2,*}, Jaime Sadhwani Alonso^{1,3}, Dunia E. Santiago García^{1,4}

(1) *Universidad de Las Palmas de Gran Canaria. Escuela de Ingenierías Industriales y Civiles. Dpto. de Ingeniería de Procesos. Campus Universitario de Tafira, 35017 Las Palmas, Spain*

(2) *Grupo Control Analítico de Fuentes Medioambientales (CAFMA), Instituto Universitario de Estudios Ambientales y Recursos Naturales (i-UNAT), Universidad de Las Palmas de Gran Canaria, 35017 Las Palmas, Spain. e-mail: jenifer.vaswani@ulpgc.es, CA.*

(3) *Grupo Sistemas Industriales de Eficiencia, Instrumentación y Protección (SEIP), Universidad de Las Palmas de Gran Canaria, 35017 Las Palmas, Spain. e-mail: jimmy.sadhwani@ulpgc.es*

(4) *Grupo de Fotocatálisis y Espectroscopia para Aplicaciones Medioambientales (FEAM), Departamento de Química, Instituto de Estudios Ambientales y Recursos Naturales (i-UNAT), Universidad de Las Palmas de Gran Canaria, 35017 Las Palmas, Spain. e-mail: dunia.santiago@ulpgc.es*

Abstract:

The use of nanomaterials in water treatment is an alternative for the development of new materials that optimize the purification process. Heterogeneous photocatalysis is used for the treatment of wastewaters contaminated with recalcitrant pollutants that cannot be removed conventionally. Ag_3PO_4 has been reported to use visible light. Another important challenge of heterogeneous photocatalysis is to find a proper support for the photocatalysts to reduce the expense associated with the separation and reuse of these materials. However, the immobilization of the catalyst leads to lower reaction rates because the surface area exposed decreases and the material used as support can also interfere. In the last years, the use of magnetic materials to support photocatalysts has attracted special attention because it allows high surface areas to be exposed. Only few authors have reported the use of Ag_3PO_4 /magnetic nanocomposites for photocatalysis and these need to be continued to improve their efficiency. In this work we synthesized Ag_3PO_4 and supported it on Fe_3O_4 .

Fe_3O_4 was synthesized at pH 12 by the addition of FeCl_3 and FeCl_2 . The magnetic material was washed with water and dried at 80°C. Ag_3PO_4 was synthesized over Fe_3O_4 from the reaction between AgNO_3 and Na_2HPO_4 . The final material was washed, recovered magnetically and dried at 80°C. For characterization, a SEM and XRD studies were carried out.

Ag_3PO_4 was synthesized and satisfactorily supported over $\text{Fe}_3\text{O}_4/\gamma\text{-Fe}_2\text{O}_3$. The photodegradation of 10 mg-L⁻¹ of methylene blue was achieved, although the apparent reaction rate constant was slightly lower for the magnetic composite than for the Ag_3PO_4 alone. This is explained because the composite contained 48% of the active Ag_3PO_4 material, as depicted from DRX studies.

Keywords:

Photocatalysis, wastewater treatment, magnetic nanomaterials,

1. Introduction

Water is a scarce resource and for many countries supply is not enough to satisfy demand. Water resources location and their quality are factors that limit their availability. This problem is further complicated by climate

change, rapid industrialization, population growth and pollution of existing water resources [1]. To solve this question different solutions are proposed which include repairing water distribution infrastructures and conservation of existing water sources. However, these options can not increase resources. Supply water can only be increased beyond hydrological cycle by desalination and water reuse. For this, a series of conventional water treatment technologies are used which include among others: ultraviolet radiation, chemical treatments, distillation and membrane processes (reverse osmosis, ultrafiltration, microfiltration, electro dialysis...), but all of them show specific disadvantages [2].

The continuous deterioration of the environment is a problem with greater relevance every day, and that requires short-term solutions. Most of the harmful contaminants found are anthropogenic compounds that have low biodegradability and therefore cannot be eliminated by conventional treatments. This is the case of the so-called emerging pollutants, which are found in low concentrations in the environment; these have the potential to carry an ecological impact, as well as adverse effects on health [3]. These contaminants include: drugs, additives, pesticides and a wide variety of compounds that, even at low concentrations, can alter endocrine functions [4] and increase the presence of resistant bacteria [5].

Elimination and control of these substances in aqueous media is complex due to their presence in large bodies of water. In recent years, emerging contaminants have been found in practically all the bodies of water studied. In Spain, among others, more than 30 emerging contaminants have been found in groundwater [6], 100 in wastewater treatment plants [7], more than 100 in wastewater already treated in conventional treatment plants [8], several in aquaculture areas [9] and 144 in river water fish [10].

Due to the nature of these contaminants, most have proven to be poorly biodegradable, and cannot be eliminated by conventional purification systems and therefore require advanced oxidation processes for their treatment [11]. Advanced oxidation processes are part of the tertiary treatment of purified water and seek to eliminate compounds that are difficult to biodegrade and reduce microbiological contamination, often with the aim of reusing the water. Among the most common tertiary processes we find ozonation, photocatalysis or membrane filtration, among others.

Based on this situation and nanotechnology development, nanomaterials use for water treatment is an alternative that allows solving drawbacks of methods traditionally used. Due to their new properties nanomaterials can contribute in obtaining stronger, lighter, cleaner and smarter surfaces and systems [12]. They have many applications ranging from automotive and aircraft (for example, reinforced and lighter materials, antifouling paints or more durable pneumatic) to biomedicine (drug released as specific organs, biosensors or prosthesis).

In water treatment, nanotechnology is finding applications through different routes [13] such as the use of large surface area of nanoparticles to adsorb contaminants (they allow retaining a higher rate of contaminants than conventional adsorbent), the use of membranes with nanomaterials (several studies have fixed nanomaterials to different polymer membranes and have obtained a greater water flow than conventional membranes) and the use of catalytic nanoparticles to decompose contaminants (nanomaterials have a higher photoactivity than conventional catalysts). Nanomaterials such as silver nanoparticles [14], TiO₂ nanoparticles and carbon nanotubes [15] have bactericidal effects that make it possible to eliminate microorganisms present in water. They also have better adsorption capacities than conventional adsorbents for low concentrations of heavy metals: porous carbon nanomaterials have been used efficiently for lead, cadmium, nickel and zinc elimination [16]. Another application is oils and organic solvents treatment: SiO₂ nanoparticles fixed to a polysulfone membrane improve antifouling properties and increase permeability from 1.08 to 17.32 l/m²·h [17]. On the other hand, boron nitride nano-slides have been shown to adsorb up to 33 times their own weight in oils and organic solvents while repelling water [18]. The use of nanomaterials has also been evaluated for emerging contaminants in water treatment: a combination of titanium dioxide nanotubes on a graphene base eliminates, with the help of the sun, traces of drugs and pesticides that escape from the current purification systems.

Of all the mentioned water treatment processes, we will focus on the use of nanomaterials in heterogeneous photocatalysis. Heterogeneous photocatalysis is used for the treatment of wastewaters contaminated with recalcitrant pollutants that cannot be removed in conventionally. One of the main drawbacks is that most photocatalysts need to be illuminated with wavelengths shorter than 388 nm [19]. Ag₃PO₄ has been reported to use visible light [20]. Another important challenge of heterogeneous photocatalysis is to find a proper support for the photocatalysts to reduce the expense associated with the separation and reuse of these materials. However, the immobilization of the catalyst leads to lower reaction rates because the surface area exposed decreases and the material used as support can also interfere [21]. In the last years, the use of magnetic materials to support photocatalysts has attracted special attention because it allows high surface areas to be

The synthesized Fe_3O_4 nanoparticles were then dispersed in distilled water, and added to the NaH_2PO_4 solution (0,15M, pH = 4.12). And then, AgNO_3 aqueous solution (0.15 M) was added with drop by drop to the above solution under continuous mechanical vibration, and then the solution was maintained at room temperature and under continuous mechanical vibration for 4 h. The magnetic material was dried at 200°C . The as-prepared $\text{Fe}_3\text{O}_4@ \text{Ag}_3\text{PO}_4$ nanoparticles were separated by an external magnetic field, The final material was washed with water to remove excess phosphate ions. The obtained $\text{Fe}_3\text{O}_4@ \text{Ag}_3\text{PO}_4$ was separated by an external magnetic field, then dried for 6 h at 80°C .

3.2. Analysis

Powder X-ray diffraction (XRD) measurements were obtained on an X-ray diffractometer PANalytical Empyrean diffractometer ($\text{Cu K}\alpha 1$, $\lambda = 1.5406 \text{ \AA}$). Crystallite sizes were estimated using the Scherrer equation and the fractions of the different phases were obtained from analysis with Match! 3@ software.

UV-vis diffuse reflectance spectra (DRS) was measured using a Varian Cary E5 spectrophotometer in the range 200 – 2000 nm.

SEM microscopic observation allowed the visualization of the ground material surface morphology. For scanning electron microscopy (SEM) measurements a Sigma 300 VP FESEM Zeiss instrument was used. It was equipped with energy dispersive X-ray spectroscopy (EDX).

3.3. Degradation experiment

The photocatalytic activities of the samples were evaluated by degradation of MB under a simulated solar lamp. A 60 W Hapro Solarium HB175 equipped with four 15 W Philips CLEO fluorescent tubes with emission spectrum from 300 to 400 nm (maximum around 365 nm) and with an average irradiation of about $90 \text{ W}\cdot\text{m}^{-2}$ was used. A photocatalyst (0.1 g) was added to an aqueous solution of MB (100 mL, 10mgL^{-1}) at room temperature in air. The suspension was magnetically stirred for 30 min in the dark to establish an adsorption desorption equilibrium to eliminate the influence of adsorption. A lamp was switched on to initiate the reaction. During irradiation, samples were taken at different time intervals for 180 min or until complete degradation was observed. Samples were centrifuged and then the decolorization of MB was measured with a UV-vis spectrophotometer (Cary 60, Varian, USA). To investigate the stability and recyclability of the as-prepared composite magnetic photocatalysts ($\text{Fe}_3\text{O}_4@ \text{Ag}_3\text{PO}_4$), recycling experiments were also performed. In the recycling experiments, after the photocatalysts were separated from the solution by an external magnetic field, the remaining solution was removed. Separated photocatalysts were washed five times with distilled water, and then used in the next degradation experiment

4. RESULTS AND DISCUSSION

4.1 Characterization

XRD was used to investigate the phase structures of the samples. Fig. 2. shows typical XRD patterns of the samples at various stages. Fig. 2 shows the XRD pattern of Fe_3O_4 nanoparticles, Fig. 2B shows the XRD pattern of Ag_3PO_4 . The successful coating and subsequent crystallization of Ag_3PO_4 and Fe_3O_4 were also confirmed (Fig. 2C).

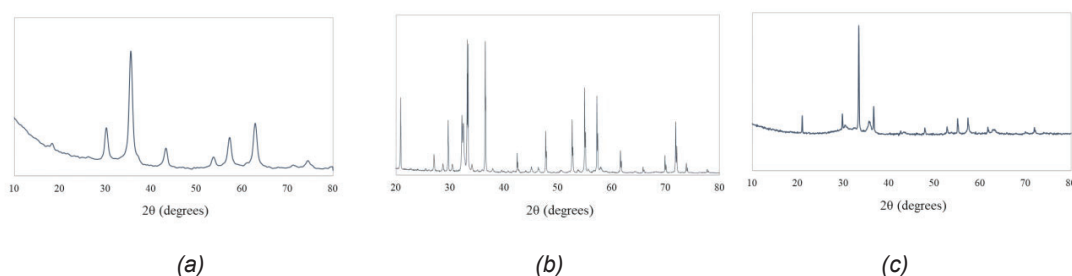


Figure 2. XRD patterns of the samples: (a) Fe_3O_4 spheres, (b) Ag_3PO_4 , (c) $\text{Ag}_3\text{PO}_4/\text{Fe}_3\text{O}_4/\gamma\text{-Fe}_2\text{O}_3$

For the Ag_3PO_4 material alone, DRX studies revealed that 100% Ag_3PO_4 was present. For the magnetic composite, the phases found in DRX studies were Ag_3PO_4 (47,8%), magnetite, Fe_3O_4 (42,6%) and maghemite, $\gamma\text{-Fe}_2\text{O}_3$ (9,5%). Although we initially synthesized Fe_3O_4 , it is known that this structure can oxidize to $\gamma\text{-Fe}_2\text{O}_3$, also magnetic, even at ambient temperature. The size of the crystals obtained from Ag_3PO_4 is 54 nm and in the case of Fe_3O_4 and $\gamma\text{-Fe}_2\text{O}_3$ crystals it is 18 nm.

Thus, the maghemite crystalline phase ($\gamma\text{-Fe}_2\text{O}_3$) can be intuited in the diffractograms of the catalysts synthesized by calcination in a nitrogen atmosphere. The formation of maghemite can occur as a consequence of the oxidation of magnetite particles, according to equation 1 [25]. This process can occur at room temperature [26], although it usually occurs more favorably in an oxidizing environment above 200 °C, with the optimum temperature for maghemite formation being between 375-400 °C [27].



The SEM image of the $\text{Ag}_3\text{PO}_4/\text{Fe}_3\text{O}_4/\gamma\text{-Fe}_2\text{O}_3$ composite is shown in Fig. 3.

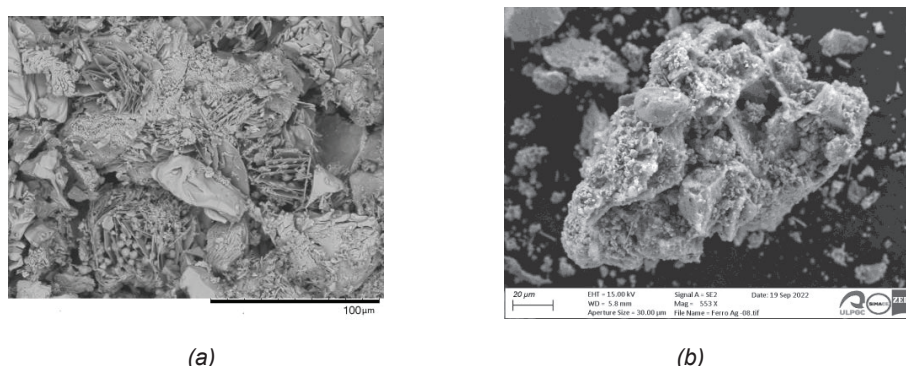


Figure 3. SEM Images of: (a) Ag_3PO_4 (b) $\text{Ag}_3\text{PO}_4/\text{Fe}_3\text{O}_4/\gamma\text{-Fe}_2\text{O}_3$

It is observed that there is a coating of silver phosphate on the ferromagnetite. Table 1 shows the elemental composition of $\text{Fe}_3\text{O}_4@\text{Ag}_3\text{PO}_4$ synthesized material.

Table 1. Composition of $\text{Fe}_3\text{O}_4@\text{Ag}_3\text{PO}_4$

Element	Weight %	Atomic %	Error %
O K	38.97	71.81	11.71
P K	9.23	8.78	7.67
Fe K	20.63	10.89	7.56
Ag L	31.17	8.52	6.87

UV-vis absorption spectra of the studied catalysts are depicted in Fig. 4. Pure Ag_3PO_4 absorbs solar energy with a wavelength shorter than approximately 500 nm. In contrast to pure Ag_3PO_4 , the absorption edge of $\text{Fe}_3\text{O}_4@\text{Ag}_3\text{PO}_4$ and Fe_3O_4 generates red shift, $\text{Fe}_3\text{O}_4@\text{Ag}_3\text{PO}_4$ and Fe_3O_4 also exhibit higher absorption in the visible region than the pure Ag_3PO_4 .

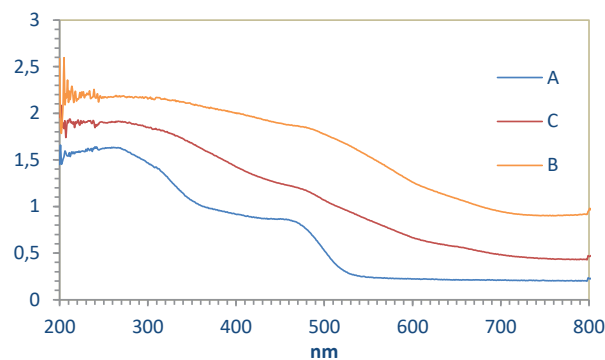


Figure 4. UV-Vis absorption spectra of: (A) pure Ag_3PO_4 , (B) pure Fe_3O_4 and (C) $\text{Ag}_3\text{PO}_4/\text{Fe}_3\text{O}_4/\gamma\text{-Fe}_2\text{O}_3$

The hysteresis curves of the magnetic materials are shown in Fig. 5. We observe that the magnetization saturation is $43 \text{ emu}\cdot\text{g}^{-1}$ for Fe_3O_4 and $15 \text{ emu}\cdot\text{g}^{-1}$ for $\text{Ag}_3\text{PO}_4/\text{Fe}_3\text{O}_4/\gamma\text{-Fe}_2\text{O}_3$.

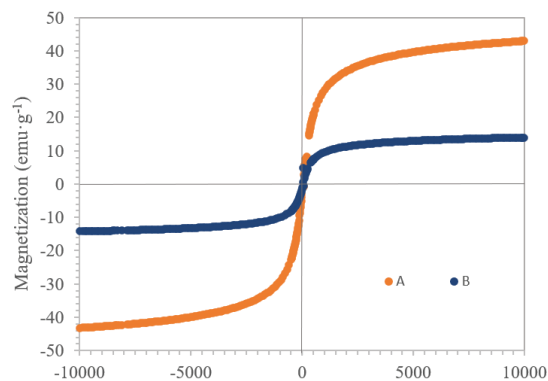


Figure 5. Hysteresis curves of: (A) Fe_3O_4 and (B) $\text{Ag}_3\text{PO}_4/\text{Fe}_3\text{O}_4/\gamma\text{-Fe}_2\text{O}_3$

4.2 Degradation Experiment

The photocatalytic degradation of MB by $\text{Fe}_3\text{O}_4@\text{Ag}_3\text{PO}_4$ under simulated solar irradiation at room temperature was investigated (Fig. 5). For comparison, the Fe_3O_4 and Ag_3PO_4 photocatalyst was also investigated. About 48% of MB was removed by $\text{Fe}_3\text{O}_4@\text{Ag}_3\text{PO}_4$ after 180 min irradiation. In contrast, pure Ag_3PO_4 exhibited the highest photocatalytic activity of the catalysts, about 96% of MB within 180 min under simulated solar irradiation.

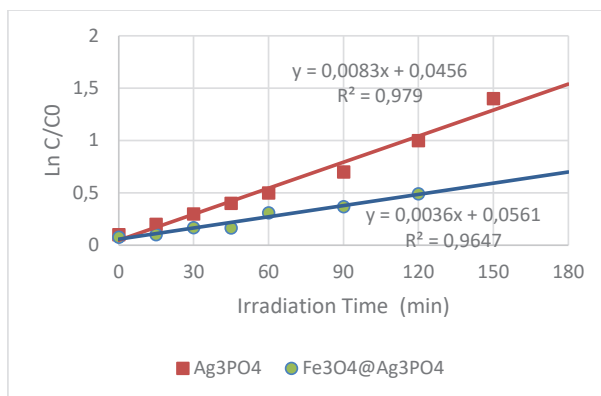


Figure 5. Photocatalytic degradation of MB over Fe₃O₄ spheres, pure Ag₃PO₄ and Fe₃O₄@Ag₃PO₄

The apparent first-order reaction rate constant for the degradation of methylene blue was 0.0077 min⁻¹ for Ag₃PO₄ and 0.0034 min⁻¹ for Ag₃PO₄/Fe₃O₄/γ-Fe₂O₃. No photolysis was observed under the studied conditions.

4.3 Separation and reuse

The recyclability of the magnetic photocatalysts was investigated. The Fe₃O₄@Ag₃PO₄ photocatalysts can be rapidly separated under an applied magnetic field in 20 s.

Fig. 6 shows the recyclability of the Fe₃O₄@Ag₃PO₄ for photocatalytic degradation of MB. The degradation activity of Fe₃O₄@Ag₃PO₄ decreased sharply only after 1 cycle. The decoloration efficiency decreased to about 32%, 25%, 19% and 14% for the 2nd, 3rd, 4th and 5th degradation cycles, respectively.

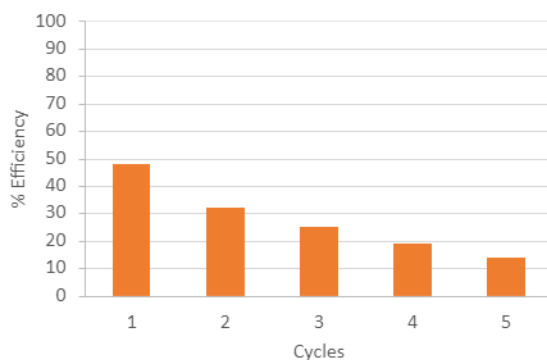


Figure 6. Recyclability of the Fe₃O₄@Ag₃PO₄

Efficiency decreases with reuse, it can be observed that the catalyst darkens due to the photocorrosion of silver by irradiation. This occurs because silver phosphate is slightly soluble in water, and silver ions can react with the generated photoelectrons reducing to elemental silver [28].

5. Conclusions

Ag₃PO₄ was synthesised and satisfactorily supported over Fe₃O₄/γ-Fe₂O₃. The photodegradation of 10 mg·L⁻¹ of methylene blue was achieved, although the apparent reaction rate constant was slightly lower for the magnetic composite than for the Ag₃PO₄ alone. This is explained because the composite contained 47.8% of the active Ag₃PO₄ material, as depicted from DRX studies.

Acknowledgments

This research was funded by Fundación Cajadecanarias and Fundación La Caixa through the project “Aplicación de nanopartículas a los procesos de tratamiento de aguas” (NAPLAGUA), with grant number 2021ECO14, Call for Research Projects 2021, with the collaboration of the company Ancor Tecnológica S.L. This project began in February 2022 until February 2024, with José Jaime Sadwani Alonso as the principal investigator.

References

- [1] Q. Zaib and H. Fath, “Application of carbon nano-materials in desalination processes,” *Desalin. Water Treat.*, vol. 51, pp. 627–636, Jan. 2012, doi: 10.1080/19443994.2012.722772.
- [2] R. Das, M. E. Ali, S. B. A. Hamid, S. Ramakrishna, and Z. Z. Chowdhury, “Carbon nanotube membranes for water purification: A bright future in water desalination.” 2014.
- [3] D. Birkholz, S. M. Stilson, and H. S. Elliott, “Analysis of Emerging Contaminants in Drinking Water - A Review,” in *Comprehensive Water Quality and Purification*, vol. 2, 2010, pp. 212–229.
- [4] C. García-Gómez, P. Gortáres-Moroyoqui, and P. Drogui, “Contaminantes emergentes: efectos y tratamientos de remoción,” *Química Viva*, vol. 10, no. 2, pp. 96–105, Mar. 2011, [Online]. Available: <https://www.redalyc.org/articulo.oa?id=86319141004>.
- [5] M. Taheran, M. Naghdi, S. K. Brar, M. Verma, and R. Y. Surampalli, “Emerging contaminants: Here today, there tomorrow!,” *Environmental nanotechnology, monitoring & management*, vol. v. 10. Elsevier B.V.
- [6] A. Jurado, E. Vázquez-Suñé, J. Carrera, M. López de Alda, E. Pujades, and D. Barceló, “Emerging organic contaminants in groundwater in Spain: a review of sources, recent occurrence and fate in a European context.,” *Sci. Total Environ.*, vol. 440, pp. 82–94, Dec. 2012, doi: 10.1016/j.scitotenv.2012.08.029.
- [7] M. J. M. Bueno, M. J. Gomez, S. Herrera, M. D. Hernando, A. Agüera, and A. R. Fernández-Alba, “Occurrence and persistence of organic emerging contaminants and priority pollutants in five sewage treatment plants of Spain: two years pilot survey monitoring.,” *Environ. Pollut.*, vol. 164, pp. 267–273, May 2012, doi: 10.1016/j.envpol.2012.01.038.
- [8] Y. Cabeza, L. Candela, D. Ronen, and G. Teijon, “Monitoring the occurrence of emerging contaminants in treated wastewater and groundwater between 2008 and 2010. The Baix Llobregat (Barcelona, Spain).,” *J. Hazard. Mater.*, vol. 239–240, pp. 32–39, Nov. 2012, doi: 10.1016/j.jhazmat.2012.07.032.
- [9] Y. Aminot *et al.*, “Environmental risks associated with contaminants of legacy and emerging concern at European aquaculture areas.” 2019, doi: 10.1016/j.envpol.2019.05.133.
- [10] Y. Pico *et al.*, “Contaminants of emerging concern in freshwater fish from four Spanish Rivers,” *Sci. Total Environ.*, vol. 659, pp. 1186–1198, 2019, doi: <https://doi.org/10.1016/j.scitotenv.2018.12.366>.
- [11] A. Gogoi, P. Mazumder, V. K. Tyagi, G. G. Tushara Chaminda, A. K. An, and M. Kumar, “Occurrence and fate of emerging contaminants in water environment,” *A Rev.*, vol. 6, pp. 169–180, Mar. 2018, doi: 10.1016/j.gsd.2017.12.009.
- [12] E. Roduner, “Size matters: why nanomaterials are different.,” *Chem. Soc. Rev.*, vol. 35 7, pp. 583–592, 2006.
- [13] A. Smith, “Opinion: Nanotech – the way forward for clean water?,” *Filtr. Sep.*, vol. 43, no. 8, pp. 32–33, 2006, doi: [https://doi.org/10.1016/S0015-1882\(06\)70976-4](https://doi.org/10.1016/S0015-1882(06)70976-4).
- [14] T. Ahmed, S. Imdad, K. Yaldram, N. M. Butt, and A. Pervez, “Emerging nanotechnology-based methods for water purification: a review,” *Desalin. Water Treat.*, vol. 52, no. 22–24, pp. 4089–4101, Jul. 2014, doi: 10.1080/19443994.2013.801789.
- [15] Q. Li *et al.*, “Antimicrobial nanomaterials for water disinfection and microbial control: potential applications and implications.,” *Water Res.*, vol. 42, no. 18, pp. 4591–4602, Nov. 2008, doi: 10.1016/j.watres.2008.08.015.
- [16] J. P. Ruparelia, S. P. Duttgupta, A. K. Chatterjee, and S. Mukherji, “Potential of carbon nanomaterials for removal of heavy metals from water,” *Desalination*, vol. 232, no. 1, pp. 145–156, 2008, doi: <https://doi.org/10.1016/j.desal.2007.08.023>.
- [17] A. L. Ahmad, M. A. Majid, and B. S. Ooi, “Functionalized PSf/SiO₂ nanocomposite membrane for oil-in-water emulsion separation,” *Desalination*, vol. 268, no. 1, pp. 266–269, 2011, doi:

<https://doi.org/10.1016/j.desal.2010.10.017>.

- [18] W. Lei, D. Portehault, D. Liu, S. Qin, and Y. Chen, "Porous boron nitride nanosheets for effective water cleaning," *Nat. Commun.*, vol. 4, no. 1, p. 1777, 2013, doi: 10.1038/ncomms2818.
- [19] C. B. Anucha, I. Altin, E. Bacaksiz, and V. N. Stathopoulos, "Titanium dioxide (TiO₂)-based photocatalyst materials activity enhancement for contaminants of emerging concern (CECs) degradation: In the light of modification strategies," *Chem. Eng. J. Adv.*, vol. 10, p. 100262, 2022, doi: <https://doi.org/10.1016/j.cej.2022.100262>.
- [20] X. Guo *et al.*, "Performance of magnetically recoverable core-shell Fe₃O₄@Ag₃PO₄/AgCl for photocatalytic removal of methylene blue under simulated solar light," *Catal. Commun.*, vol. 38, pp. 26–30, 2013, doi: <https://doi.org/10.1016/j.catcom.2013.04.010>.
- [21] D. E. Santiago, M. R. Espino-Estévez, G. V. González, J. Araña, O. González-Díaz, and J. M. Doña-Rodríguez, "Photocatalytic treatment of water containing imazalil using an immobilized TiO₂ photoreactor," *Appl. Catal. A Gen.*, vol. 498, pp. 1–9, 2015, doi: <https://doi.org/10.1016/j.apcata.2015.03.021>.
- [22] E. Abroshan, S. Farhadi, and A. Zabardasti, "Novel magnetically separable Ag₃PO₄/MnFe₂O₄ nanocomposite and its high photocatalytic degradation performance for organic dyes under solar-light irradiation," *Sol. Energy Mater. Sol. Cells*, vol. 178, pp. 154–163, 2018, doi: <https://doi.org/10.1016/j.solmat.2018.01.026>.
- [23] Z. Liu *et al.*, "The triple-component Ag₃PO₄-CoFe₂O₄-GO synthesis and visible light photocatalytic performance," *Appl. Surf. Sci.*, vol. 458, pp. 880–892, 2018, doi: <https://doi.org/10.1016/j.apsusc.2018.07.166>.
- [24] B. Lv, Y. Xu, H. Tian, D. Wu, and Y. Sun, "Synthesis of Fe₃O₄/SiO₂/Ag nanoparticles and its application in surface-enhanced Raman scattering," *J. Solid State Chem.*, vol. 183, no. 12, pp. 2968–2973, 2010, doi: <https://doi.org/10.1016/j.jssc.2010.10.001>.
- [25] S. Laurent *et al.*, "Magnetic Iron Oxide Nanoparticles: Synthesis, Stabilization, Vectorization, Physicochemical Characterizations, and Biological Applications," *Chem. Rev.*, vol. 108, no. 6, pp. 2064–2110, Jun. 2008, doi: 10.1021/cr068445e.
- [26] A. Haneda, K. & Morrish, "Magnetite to maghemite transformation in ultrafine particles.," *J. Phys. Colloq.*, vol. 38, pp. 321–323, 1977, doi: <https://doi.org/10.1051/jphyscol:1977166>.
- [27] H. Lepp, "Stages in the oxidation of magnetite," *Am. Mineral.*, vol. 42, pp. 679–681, 1957.
- [28] X. Chen, Y. Dai, and X. Wang, "Methods and mechanism for improvement of photocatalytic activity and stability of Ag₃PO₄: A review," *J. Alloys Compd.*, vol. 649, no. C, pp. 910–932, 2015, doi: [10.1016/j.jallcom.2015.07.174](https://doi.org/10.1016/j.jallcom.2015.07.174).